(Received 24 December 2025, Accepted 22 January 2026, Scheduled 18 March 2026)

A High-Sensitivity Microwave Patch Sensor for Olive Oil Adulteration Detection

Cheng Chen and Shen-Yun Wang*

Research Center of Applied Electromagnetics, Nanjing University of Information Science and Technology, Nanjing 210044, China

ABSTRACT: In this paper, a highly sensitive microwave patch sensor for detecting adulteration in olive oil is proposed. First, a broadband electromagnetic property of olive oil adulterated with corn oil is characterized by using a Cole-Cole function. Next, a microwave patch sensor is designed with a circular patch integrated with a meandered slot and a complementary split ring resonator (CSRR) in the ground plane. A prototype of the microwave patch sensor is fabricated to detect the adulterant in olive oil. The results indicate that the proposed microwave patch sensor can detect the adulteration ratio of corn oil in the parent olive oil ranging from 0 to 100%. The sensitivity, resonance frequency shift, and quality factors are 6.16%, 41 MHz, and 173, respectively. The proposed microwave patch sensor maintains a simple structure and an electrically small size ($ka = 0.83$), high sensitivity, low cost, and ability to fast detect adulterants for olive oil.

1. INTRODUCTION

Extra virgin olive oil (EVOO) is obtained directly from olive fruit through physical cold pressing. The beneficial health effects of olive oil intake are attributed to the high content of monounsaturated fatty acids, such as oleic acid, which have a great ability to protect against cardiovascular events, improve inflammation, and prevent neurodegenerative diseases [1]. However, given the high economic value, limited production, and substantial demand, the risk of adulteration of olive oil is significantly elevated. Therefore, it is necessary to develop a rapid and effective method to detect adulterants in olive oil. Common chemical analyses of EVOO include gas liquid chromatography (GLC) [2] and liquid chromatography tandem mass spectrometry (LC-MS/MS) [3]. However, chromatographic techniques are known to be labor-intensive, time-consuming, and often require extensive sample preparation and reagent use, consequently resulting in environmental stress.

Many physical techniques based on optical, magnetic, or electrical signals of the sample under test (SUT) have been developed for the rapid determination of adulteration in edible oils. Optical techniques include the use of various spectroscopic methods, such as Raman spectroscopy [4], infrared spectroscopy [5], and fluorescence spectroscopy [6]. Moreover, other physical methods using nuclear magnetic resonance [7], electronic tongue [8], and capacitive sensing [9] have been reported. These techniques are typically coupled with chemometric methods and offer an alternative approach for detecting adulterants in EVOO. However, it should be pointed out that the above-mentioned techniques usually depend on expensively testing the equipment, involve extensive sample preparation, and are impractical for in situ analysis owing to the size of the equipment. For capacitive sensors, regular calibration is necessary to account for the influence of environmental factors, such as temperature, humidity, and surrounding objects.

In comparison, microwave sensing approaches based on dielectric spectroscopy have garnered tremendous attention, and they are widely applied in the quality detection of oils [10], liquid concentration analysis [11], soil moisture monitoring [12], blood glucose sensing [13], and some other sensing applications [14, 15], given the advantages of real-time operation, low cost, good repeatability, and high robustness. The sensing principle is based on the fact that the relative permittivity of the SUT is sensitive to changes in its composition in the microwave frequency range.

Microwave sensors can be categorized according to different classification criteria [16–18]. On the one hand, based on the application method, microwave sensors can be classified into two categories: submersible sensors [19, 23] and non-submersible sensors, namely microfluidic sensors [24–29] and sensors figured by transmission lines loaded with specific microwave resonators [30–36]. However, the channels in microfluidic sensors are susceptible to contamination and irreversible clogging due to the viscosity of the oil under test, which may increase the uncertainty or error of the measurement [27]. Microwave sensors composed of transmission lines and resonators typically require a dedicated sample holder [32, 33]. On the other hand, microwave sensors can be categorized by their resonator structures, such as split-ring resonator (SRR) [20, 36], complementary SRR (CSRR) [19, 31], interdigital capacitor (IDC) [33], and fractal geometries [34].

Sensors based on CSRR or SRR structures are known for their high sensitivity and are widely used for sensing the permittivity of liquids. The primary advantage of CSRR and SRR lies in their distributed capacitance across the entire structure, which renders the resonant frequency highly responsive to variations in the dielectric constant of the sample under test

* Corresponding author: Shen-Yun Wang (wangsy2006@126.com).

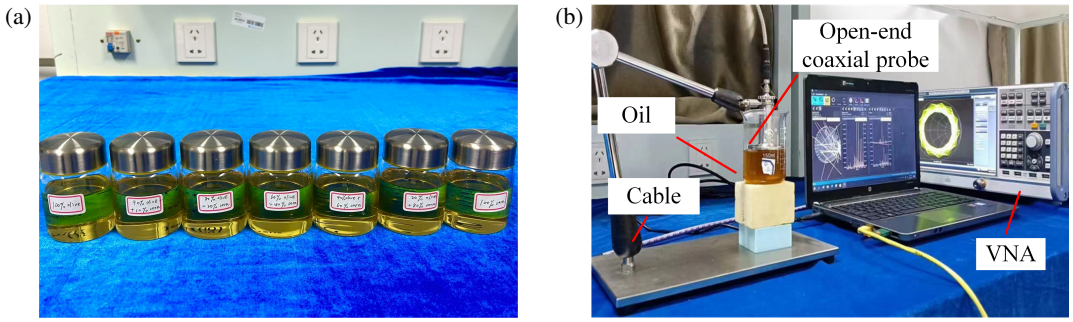

FIGURE 1. (a) Experimental oil samples, and (b) experimental setup of the oil dielectric measurement apparatus.

(SUT). Among others, meander-slot-loaded CSRRs have attracted significant research attention for diverse applications, such as permittivity measurement [37] and concentration analysis [39]. Studies indicate that such meander-slot-like structures can achieve higher sensitivity while also lowering the resonance frequency in permittivity detection [38]. By incorporating the meander-slot structure into the CSRR, the electric field confinement is improved, which leads to a substantial enhancement in detection sensitivity, as demonstrated by simulations in [37].

Taking these factors into account, a submersible microwave sensor with probes immersed inside the SUT has been widely investigated [19–23]. A complementary split ring resonator (CSRR) loaded planar microwave probe with improved sensitivity was proposed for liquid adulteration detection in [19]. A submersible printed SRR-based sensor for the detection of relative permittivity of solid and liquid materials is proposed in [20]. Two planar submersible resonance sensors for measuring permittivity and identifying adulteration in vegetable oils were presented in [21]. A compact multifunctional five-wire line-based microwave sensor for volumetric characterization of liquids was reported in [22]. In [23], a microwave resonator-based sensor in the shape of a spiral was presented, and a feedforward neural network was used to assess the authenticity of the EVOO.

Recent investigations have concentrated on the high sensitivity, compact size, and convenience of submersible sensors. Few studies have explored dielectric spectroscopy for edible oils, making it difficult to mitigate the influence of environmental factors, particularly temperature, on the detection accuracy of microwave sensing.

In this study, a microwave patch sensor is proposed for the real-time detection of adulterants in olive oil. Compared with existing microwave sensors, the proposed design distinguishes itself in two key aspects. First, it employs the Cole-Cole function, parameterized by the concentration of adulterants in olive oil, enabling direct concentration sensing via simple immersion of the sensor into the oil sample. Second, the integration of a meander slot with the CSRR structure achieves a larger detection range and higher sensitivity, which is attributed to the high-quality factor (Q-factor), which enhances the performance of the microwave patch sensor. Additionally, the sensor is compact, low-cost, and easy to fabricate.

The remainder of this paper is organized as follows. In Section 2, the structure of the microwave patch sensor and its equivalent circuit model are presented. The simulated and experimental results are presented in Section 3. In Section 4, the performance of the proposed sensor is evaluated. The conclusions are presented in Section 5.

2. MATERIALS AND DESIGN OF ANTENNA SENSOR

2.1. Sample Preparation and Dielectric Measurement

The broadband dielectric property of adulterated olive oil must be characterized to design a microwave sensor for the adulterant detection in olive oil. To obtain the permittivity function of the adulterated olive oil, seven mixed oil samples were prepared by adding corn oil to the parent olive oil, where the corn oil concentrations were set to 0%, 10%, 20%, 40%, 60%, 80%, and 100% (v/v), respectively, as shown in Fig. 1(a). Corn and olive oils are commercially available products and purchased from local supermarkets. They have a fresh shelf life to ensure their natural properties and antioxidant characteristics. The dielectric properties of the mixed oil can be described using the complex permittivity:

$$\hat{\varepsilon}(\omega) = \varepsilon'(\omega) - \mathrm{j}\varepsilon''(\omega) \tag{1}$$

where ω is the angular frequency, and j is the imaginary unit. The real part $\varepsilon'(\omega)$ is the dielectric constant, which represents a measurement of the polarizability of the mixed oil, where the imaginary part $\varepsilon''(\omega)$ represents the dielectric loss.

Next, the dielectric properties of the mixed oil samples were measured using a vector network analyzer (ZNB20, Rohde & Schwarz) and an 85070E open coaxial probe kit (DAK-12, Keysight) via the coaxial reflection method. The experimental setup is shown in Fig. 1(b). The reflection coefficients are measured by immersing the coaxial probe in mixed oil samples stored in beakers. The measurements were performed over a frequency range of 20–3000 MHz with a step of 20 MHz. To reduce the influence of random errors, the complex permittivity of each mixed oil sample was measured 10 times at room temperature (25°C), and the average value was used to determine the dielectric properties.

The measured complex permittivity of the seven mixed oil samples is shown in Fig. 2. The dielectric constant and loss are plotted in Figs. 2(a) and 2(b), respectively. It is observed

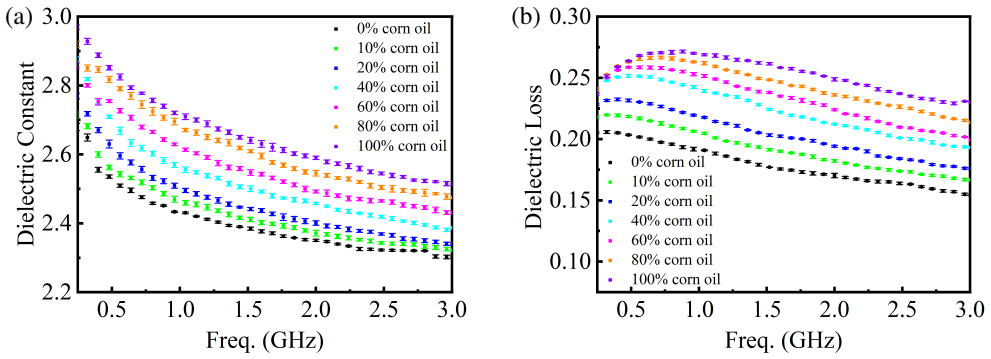

FIGURE 2. Dielectric properties of olive oil with different adulteration ratios of corn oil: (a) dielectric constant, (b) dielectric loss.

that the dielectric constant of the mixed oil sample with a given adulteration concentration of corn oil decreases when the frequency increases from 20 MHz to 3000 MHz. Meanwhile, the dielectric loss increases with an increase in frequency in the lower frequency range and decreases with the increase of frequency in the higher frequency band. In comparison, the dielectric constant of olive oil is lower than that of corn oil. This feature is attributed to the difference in unsaturated fatty acid content between olive oil and corn oil [40]. The linolenic acid (LNA) content in corn oil is known to be higher than that in olive oil. Because the LNA has a larger degree of unsaturation with higher polarizability, the dielectric constant of the mixed oil sample increases as increasing the degree of unsaturation or the concentration of corn oil.

2.2. Cole-Cole Function of the Mixed Oil

The polarizability arises from the synergistic effect of intermolecular interactions, whereas the dielectric loss primarily originates from the dipole relaxation process. Dielectric loss mainly arises from dipole relaxation, which occurs at microwave frequencies [41]. For a mixed oil sample, the resulting complex permittivity can be characterized by a single-order Cole-Cole function [42].

$$\hat{\varepsilon}(\omega) = \varepsilon_\infty + \frac{\varepsilon_s - \varepsilon_\infty}{1 + (\mathrm{j}\omega\tau)^{1-\alpha}} - \mathrm{j}\frac{\sigma}{\varepsilon_0\omega} \tag{2}$$

where ε_∞ is the dielectric constant at infinitely high frequencies; ε_s, τ, and α represent the static permittivity, relaxation time, and dispersion parameter of the mixed oil solution, respectively; ε_0 is the permittivity of free space, with a value of 8.854×10^{-12} F/m. Finally, σ represents the ionic conductivity of the mixed-oil solution. Edible oils can be neglected as there are no ions in the plant oil.

Based on the measured dielectric constant and dielectric loss, a MATLAB fitting program that employs particle swarm optimization (PSO) was developed to obtain the best-fitting parameters in the Cole-Cole function. The fitted parameters for olive oil with different adulteration ratios of corn oil, defined as the volume fraction of corn oil in the parent olive oil, are shown in Table 1.

Subsequently, the obtained Cole-Cole parameters were fitted using quadratic polynomials through the least squares method,

TABLE 1. Fitting parameters of the single-order Cole-Cole model of olive oil with different adulteration ratio.

Adulteration ratio (%)	ε_∞	ε_s	τ (ps)	α
0	2.0729	3.1634	538.45	0.5775
10	2.1104	3.1876	417.47	0.5128
20	2.1563	3.2105	394.45	0.4933
40	2.1892	3.2469	320.27	0.4725
60	2.2055	3.2701	272.56	0.4427
80	2.242	3.2921	226.61	0.4322
100	2.2761	3.3015	188.73	0.4248

and the quadratic polynomials related to the adulteration ratio V are expressed as

$$\varepsilon_\infty(v) = -1.045 \times 10^{-5}v^2 + 0.0029v + 2.0837 \tag{3}$$

$$\varepsilon_s(v) = -1.1 \times 10^{-5}v^2 + 0.0025v + 3.1642 \tag{4}$$

$$\tau(v) = 0.02619v^2 - 5.705v + 506.8805 \tag{5}$$

$$\alpha(v) = -1.771 \times 10^{-5}v^2 - 0.0031v + 0.5593 \tag{6}$$

By substituting the calculated parameters into the Cole-Cole function, the real and imaginary parts of the complex permittivity of the mixed oil with a specific adulteration ratio are obtained as follows:

$$\varepsilon'(\omega) = \varepsilon_0\left(\varepsilon_\infty(v) + \frac{\varepsilon_s(v) - \varepsilon_\infty(v)}{1 + (\omega\tau(v))^2}\right) \tag{7}$$

$$\varepsilon''(\omega) = \frac{\varepsilon_0\omega\tau(v)\left(\varepsilon_s(v) - \varepsilon_\infty(v)\right)}{1 + (\omega\tau(v))^2} \tag{8}$$

By setting the adulteration ratio of corn oil to 10%, 20%, 40%, 60%, 80%, and 100%, the corresponding Cole-Cole parameters can be calculated using Eq. (3) to Eq. (6). Next, these parameters were substituted into Eqs. (7) and (8), and the fitting curves of the dielectric constant and dielectric loss versus frequency are plotted in Figs. 3(a) and (b), respectively. It was found that the fitting curves obtained using the Cole-Cole function match well with the measured ones, where the coefficient of determination (R^2) was larger than 0.991.

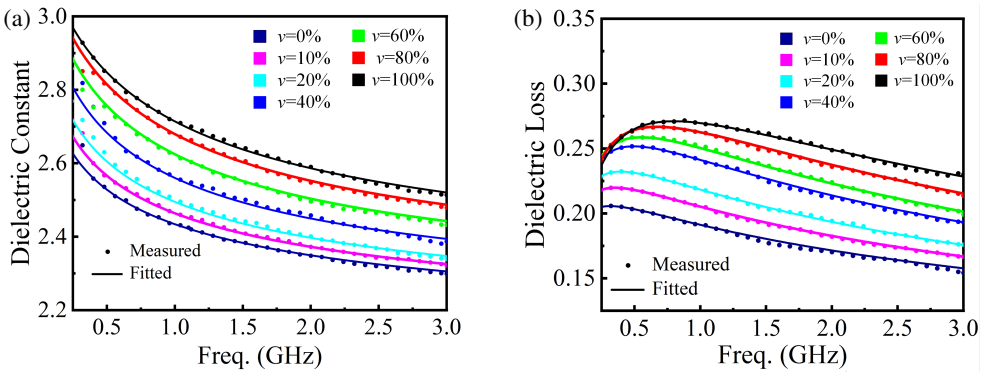

FIGURE 3. Reconstruction of dielectric properties for three mixed-oil samples using the single-order Cole-Cole function: (a) dielectric constant, (b) dielectric loss.

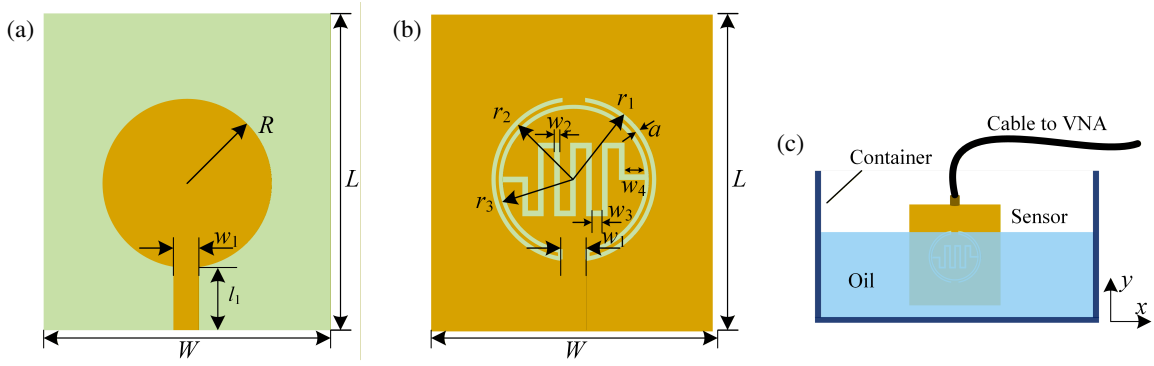

FIGURE 4. The structure of the microwave patch sensor: (a) top view, (b) bottom view, and (c) 3D view in the olive oil sample.

2.3. Design of the Microwave Patch Sensor

Using the Cole-Cole function of the mixed oil, a circular patch-based microwave sensor is designed, which consists of a circular patch on the top of a substrate and a meandered slot-loaded CSRR (MS-CSRR) integrated in the ground plane on the bottom of the substrate. The top and bottom geometric patterns of the microwave patch sensor are shown in Figs. 4(a) and (b), respectively. The circular patch antenna is fed with a microstrip line. The dielectric substrate is FR4 with a relative dielectric constant of 4.4, loss tangent of 0.02, and thickness of 0.8 mm. It should be noted that the structure of the microwave patch sensor is optimized by immersing it inside pure olive oil at room temperature, as shown in Fig. 4(c).

In the design process, the microwave patch sensor loaded with pure olive oil was structurally optimized using Computer Simulation Technology (CST) Microwave Studio 2022. It was found that the width of the ring of the CSRR a and the width of the meandered slot w_2 have a significant impact on the performance of the microwave patch sensor. The reflection coefficients for different values of a and w_2 are shown in Figs. 5(a) and (b), respectively. Results indicate that a very sharp reflection notch appears in $|S_{11}|$ when $a = 0.25$ mm and $w_2 = 0.3$ mm. In this work, the microwave patch sensor is designed to work around 2.4 GHz under the tradeoff between the sensor size and fabrication cost, and the final optimized geometrical parameters denoted in Figs. 4(a) and (b) are listed in Table 2.

TABLE 2. Geometrical parameters of the microwave patch sensor.

Parameter	Value (mm)	Parameter	Value (mm)
L	21.5	w_1	1.5
W	18.6	w_2	0.30
R	5.50	w_3	0.40
r_1	4.75	w_4	1.65
r_2	4.15	w_5	1.40
r_3	4.00	a	0.25
l_1	4.25	h	0.8

The MS-CSRR structure was designed to increase the electrical and magnetic energy storage of the circular patch by introducing additional capacitance and inductance. As a result, the microwave patch sensor had an electrically small size ($ka = 0.83$) and a high-quality factor. The Q factor of the proposed microwave sensor was calculated by using the following formula:

$$Q = f_0/f_{3\,\mathrm{dB}} \tag{9}$$

where f_0 is the resonance frequency, and $f_{3\,\mathrm{dB}}$ is the 3.0 dB bandwidth measured by $|S_{11}|_{\min}+3.0$ dB. The calculated Q factor of the optimized microwave patch sensor is approximately 173.

The design of the microwave patch sensor can be divided into three stages, as illustrated in Fig. 6. In stage 1, a circular CSRR was etched in the ground plane, and a reflection

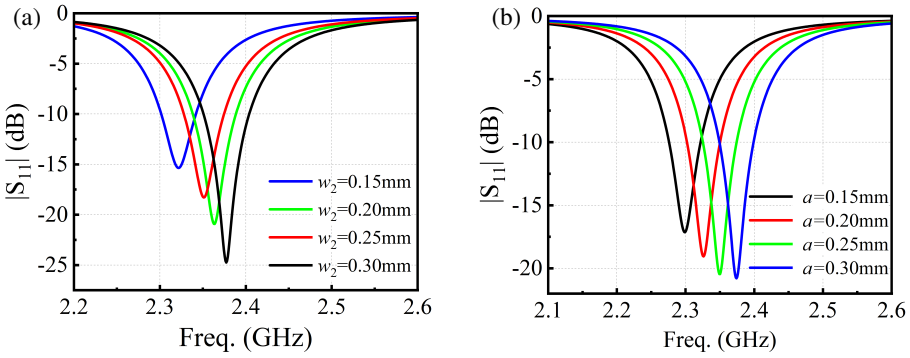

FIGURE 5. The reflection coefficient of the microwave patch sensor with different (a) width of the meandered slot, and (b) width of the CSRR ring.

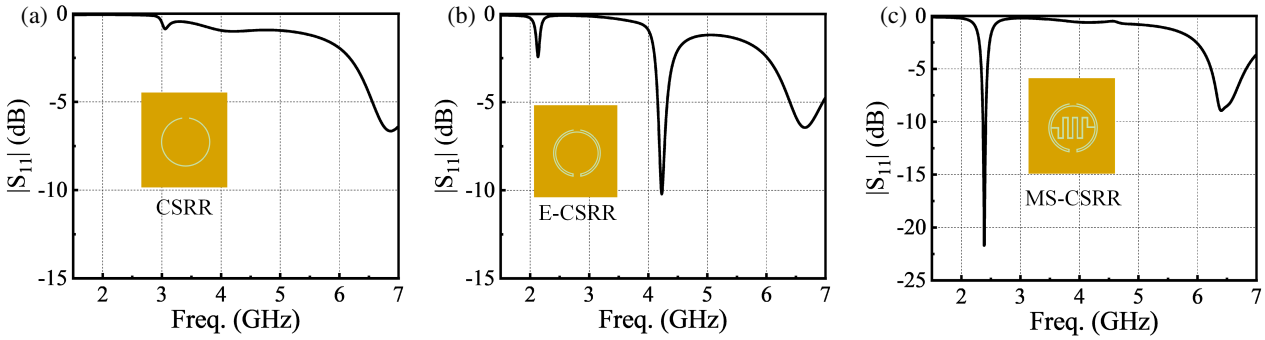

FIGURE 6. Simulated reflections of the proposed sensor integrated with (a) CSRR, (b) E-CSRR, and (c) MS-CSRR in the ground plane.

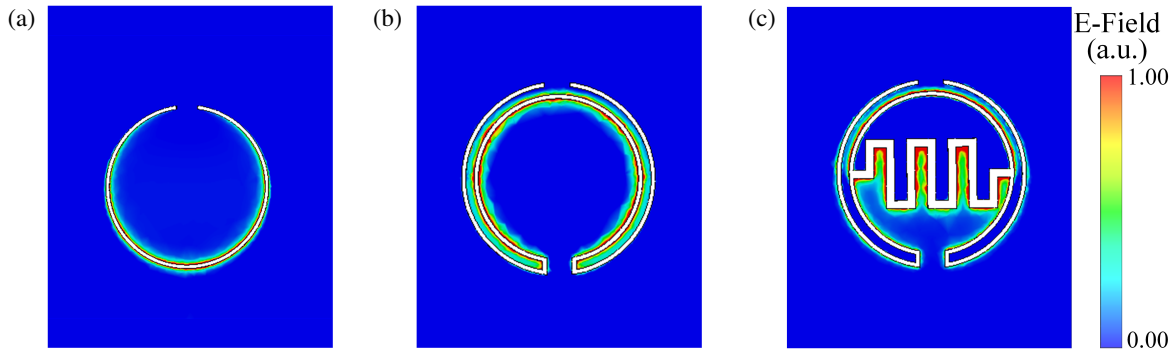

FIGURE 7. Electric field distributions on the ground plane of the microwave patch sensor integrated with (a) CSRR, (b) E-CSRR, and (c) MS-CSRR at their resonance frequency.

notch at 6.87 GHz with a notch depth of 6.65 dB takes place, as shown in Fig. 6(a). In stage 2, an extended CSRR (E-CSRR) was designed by adding another ring slot to the circular CSRR. The approach causes the CSRR to have a smaller electrical size by increasing the inductance. As a result, the reflection notch moves to 4.22 GHz, and the notch depth increases to 10.22 dB due to the increased inductance, as shown in Fig. 6(b). In stage 3, to increase both the electrical and magnetic energy storages, a meandered slot was added to the E-CSRR designed in stage 2 and a sharp reflection notch at 2.38 GHz with a notch depth of 21.73 dB was obtained, as shown in Fig. 6(c). Compared with the CSRR and E-CSRR designed in stages 1 and 2, the proposed microwave patch sensor integrated with MS-CSRR in the ground plane has a maximum Q factor as the electrical and magnetic energy storage is increased by introducing the meandered slot.

To obtain an insight into the energy storage, the electric field distribution on the MS-CSRR is compared with that on the

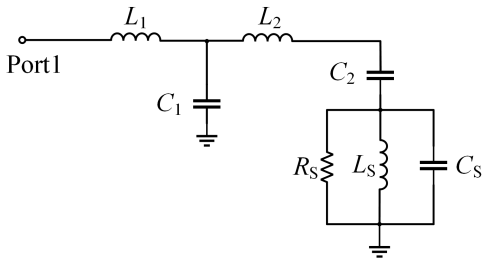

FIGURE 8. Equivalent circuit model of the proposed microwave patch sensor.

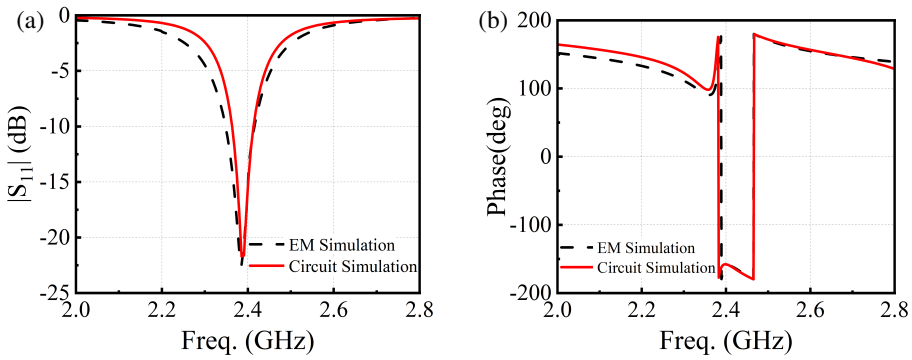

FIGURE 9. Comparison between the circuit model and full-wave electromagnetic simulation: (a) magnitude, and (b) phase of the S_{11}.

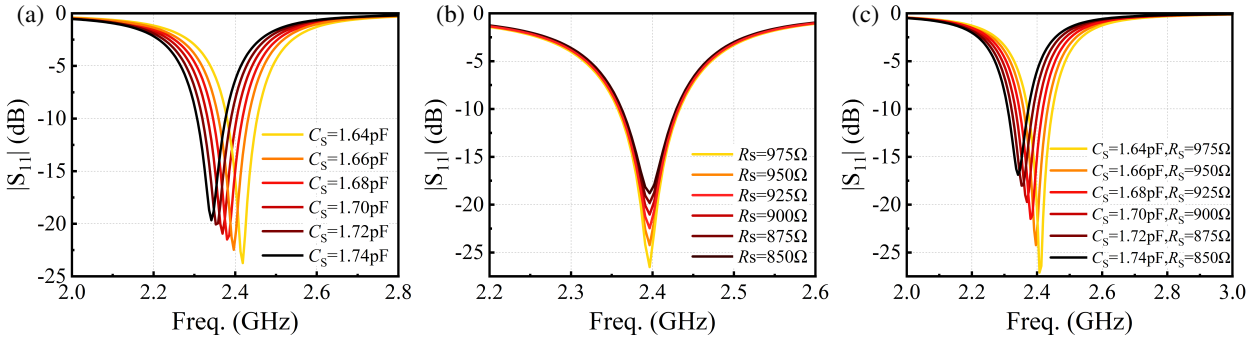

FIGURE 10. Reflection of the microwave patch sensor: (a) $|S_{11}|$ with different values of C_S, (b) $|S_{11}|$ with different values of $R_S S$, and (c) $|S_{11}|$ with different values of C_S and R_S.

CSRR and E-CSRR, as shown in Figs. 7(a) to (c). It is evident that a higher electric field confinement is achieved in the MS-CSRR structure, where the electric field energy is mainly concentrated around the meandered slot, as shown in Fig. 7(c). In general, a high electric field density makes the meandered slot very sensitive to the dielectric variation of the oil under testing. Consequently, the MS-CSRR-based sensor has a better sensitivity than the other sensors.

The equivalent circuit model of the designed microwave patch sensor is shown in Fig. 8. In this model, L_1 and C_1 are used to characterize the microstrip line; L_2 and C_2 represent the original inductance and capacitance of the patch without the MS-CSRR; L_S, C_S, and R_S represent the additional inductance, capacitance, and resistance caused by the MS-CSRR integrated in the ground plane. Finally, the resonance frequency of the microwave patch sensor is given by

$$f_0 = \frac{1}{2\pi\sqrt{L_S(C_S + C_2)}} \tag{10}$$

$$f_0 \propto \frac{1}{\sqrt{C_S}} \propto \frac{1}{\sqrt{C_{0S}\varepsilon_r}} \propto \frac{1}{\sqrt{\varepsilon_r}} \tag{11}$$

where C_{0S} represents the capacitance of the sensor located in free space, and ε_r is the dielectric constant of the oil sample under test. It can be seen that the resonance frequency is inversely proportional to the square root of the effective capacitance of the sensor or dielectric constant of the oil sample. In other words, when the microwave sensor is immersed into oil sample contained in the beaker, the capacitance of the sensor

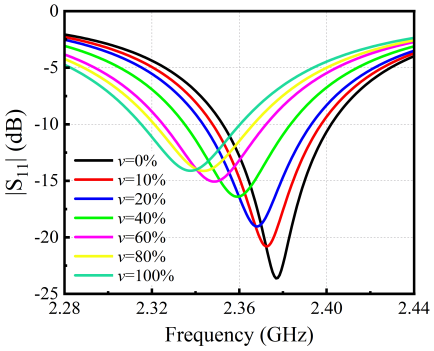

FIGURE 11. The simulated reflections of the mixed oil for different adulteration ratios of corn oil.

will increase as more electric energy is stored in the volume of the oil sample.

Next, the equivalent circuit of the microwave patch sensor was simulated using lumped circuit methods, and the results were compared with those obtained using full-wave electromagnetic simulations, as shown in Figs. 9(a) and (b). The magnitude and phase of S_{11} are in good agreement, and a sharp phase change occurs at the resonance of the proposed sensor.

The influence of the effective circuit parameters on the notch depth and resonance frequency in reflection ($|S_{11}|$) was investigated, as shown in Figs. 10(a) and (b). The resonance frequency (the reflection notch in $|S_{11}|$) gradually decreased as C_S increased; however, the amplitude remained almost unchanged, as shown in Fig. 10(a). Therefore, C_S mainly affects the resonance frequency, which is associated with the dielectric con-

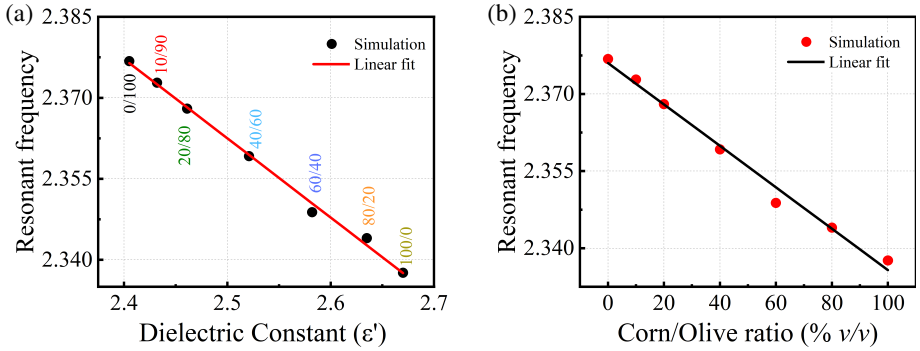

FIGURE 12. The simulated resonance frequency of the microwave patch sensor versus (a) the dielectric constant of mixed oil, and (b) adulteration ratio of corn oil.

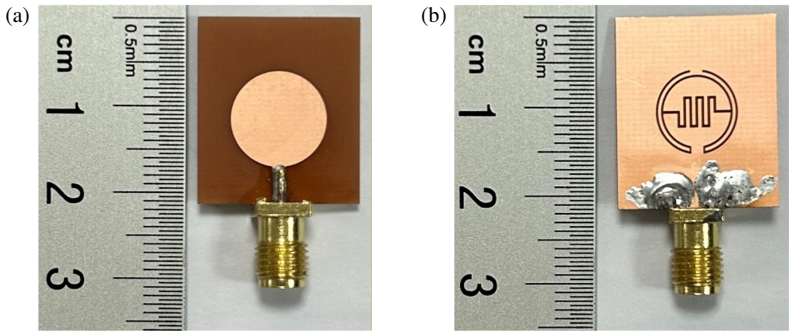

FIGURE 13. Photograph of proposed microwave patch sensor: (a) top view, and (b) bottom view.

stant of the mixed oil sample. The amplitude of the reflection notch decreased as R_S increased, as shown in Fig. 10(b). Thus, the R_S affects the amplitude of the resonance frequency, which is partly determined by the dielectric loss of the mixed oil. When the microwave patch sensor was immersed in adulterated olive oil, both the C_S and R_S changed with the adulteration ratio of corn oil. In this case, both the resonance frequency and its notch depth change, as shown in Fig. 10(c).

3. RUSELTS

3.1. Simulation Results

To validate the performance of the proposed microwave patch sensor for adulterant detection in olive oil, reflections were simulated when olive oil was adulterated with different volumes of corn oil, as shown in Fig. 11. The adulteration ratio of corn oil was set to range from 0 to 100%, and the resonance frequency ranged from 2.34 to 2.38 GHz. The resonance frequency significantly decreased with an increase in the adulteration ratio. This is due to the increase in both the dielectric constant and dielectric loss of the mixed oil when the corn oil content is increased, leading to a larger effective capacitance and a smaller resistance in the equivalent circuit model. Consequently, the resonance frequency shifts to a lower frequency with a smaller notch depth.

The resonance frequency versus the dielectric constant of the mixed oil and the adulteration ratio of corn oil are shown in Figs. 12(a) and (b), respectively. A linear fitting equation was set up to reveal the relationship between the resonance frequency and dielectric constant, which is given as:

$$f_0 = 2.7294 - 0.1467 \cdot \varepsilon'(\omega) \tag{12}$$

where the coefficient of determination was 0.997. In addition, a linear fitting equation was developed to reveal the relationship between the resonance frequency and the adulteration ratio of corn oil in the mixed oil, which is given as:

$$f_0 = 2.376 - 4.025 \times 10^{-4} \cdot v \tag{13}$$

where the coefficient of determination was 0.989. Hence, when the resonance frequency is measured, the dielectric constant and adulteration ratio of corn oil in the mixed oil can be calculated by using Eqs. (12) and (13), respectively:

3.2. Experimental Results

A prototype was fabricated for adulterant detection in olive oil to validate the design of a microwave patch sensor. Photographs of the fabricated microwave patch sensor are shown in Fig. 13. Next, the microwave patch sensor, together with an SMA connector, was fully immersed in the olive oil under test to detect the adulteration ratio of the corn oil. It should be pointed out that the oil container was sufficiently large to eliminate reflection from the sample border.

The experimental setup is shown in Fig. 14, where the microwave patch sensor is connected to a vector network analyzer (VNA, ZNB20, Rohde & Schwarz) using an RF cable, and the reflection can be measured. Four mixed oil samples with corn oil adulteration ratios of 0%, 20%, 40%, and 80% were placed in four clean beakers. The microwave patch sensor was

TABLE 3. Comparison of the proposed microwave sensor versus state-of-the-art microwave sensors.

Ref. No.	Sensor Structure	Application Sensing	f_0 (GHz)	Sensing Parameter	Detection Range	Max Sensitivity (%)	Electrical Size (ka)	Substrate
[19]	Double CSRR	Edible Oils	11.56	S_{11}	0%–100%	9.8	2.99	Roger 5880
[21]	Shorted SRR	Solid and Liquid	2.4	S_{11}	NA	2.59	0.96	FR4 epoxy
[27]	Star-slotted patch	Edible Oils	2.68	S_{11}	NA	1.87	2.78	FR4 epoxy
[29]	Spiral-SLSP	Edible Oils	0.36	S_{11} and S_{21}	NA	0.80/8.5	0.23	Rogers 5880
[30]	Metamaterial	Edible Oils	8–12	S_{11}	0%–100%	0.56	2.67	FR4 epoxy
[33]	DG-IDC	chemical liquids	4.065	S_{21}	NA	3.5	1.80	FR4 epoxy
T. W	MC-CSRR	Oil	2.8	S_{11}	0%–100%	6.16	0.83	FR4 epoxy

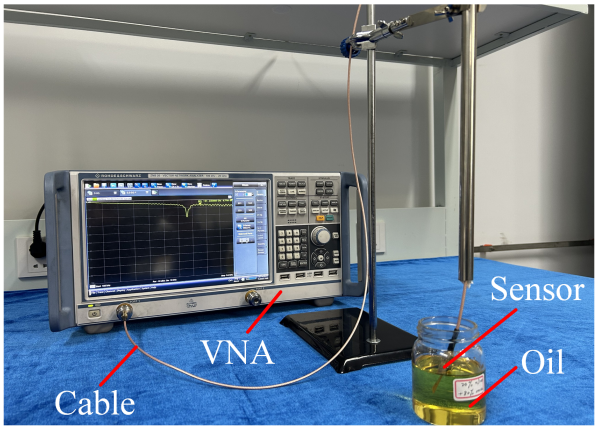

FIGURE 14. Experimental setup of the detection of adulteration of corn oil in olive oil.

fixed to a mounting bracket to minimize cable movement for repeatable measurements. The measured reflections are shown in Fig. 15 for the four olive oil samples with different corn oil adulteration concentrations. The measured resonance frequencies were consistent with the simulation results. The slight difference in the resonance frequency is caused by the fabrication tolerance. Hence, when the resonance frequency is measured, the adulteration ratio of corn oil to the parent olive oil can be determined using Eq. (13).

Additionally, the repeatability of notch depth $|S_{11}|_{\min}$ and resonance frequency were investigated by performing 10 repeated measurements. The mean $|S_{11}|_{\min}$ and resonance frequency have been plotted against different corn oil adulteration ratios, as shown in Fig. 16. The measurement uncertainty is illustrated by error bars denoting the standard deviation. The relative measurement error for the resonant frequency was below 0.12%, whereas that for $|S_{11}|_{\min}$ was below 2.3%. The small relative standard deviation demonstrates the stable performance and reliability of the proposed microwave patch sensor.

4. DISCUSSIONS

In this study, a microwave patch sensor integrated with an MS-CSRR in the ground plane was designed and fabricated for adulterant detection in the parent olive oil. Compared with tradi-

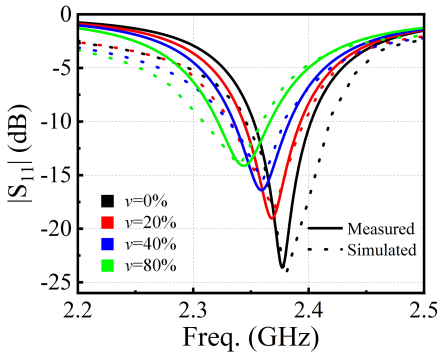

FIGURE 15. Measured and simulated reflections of the microwave patch sensor immersed in the mixed oil samples with adulteration ratios of corn oil of 0%, 20%, 40%, and 80%.

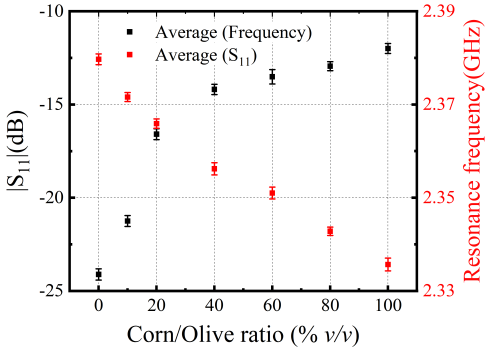

FIGURE 16. Repeatability analysis showing minimal variation in frequency response across repeated measurements.

tional patch antenna-based microwave sensors, the proposed sensor features a higher sensitivity for adulterant detection in olive oil and an electrically small size.

The relative sensitivity ($S\%$) of the microwave patch sensor is defined as the ratio of the resonance shift to the change in the dielectric constant and is given as follows:

$$S(\%) = \frac{f_{mix} - f_{OO}}{f_{OO} \cdot (\varepsilon'_{mix} - \varepsilon'_{OO})} \times 100 = \frac{\Delta f}{f_{OO} \cdot \Delta\varepsilon'} \times 100 \quad (14)$$

where f_{mix} and f_{OO} are the resonance frequencies of the microwave patch sensor immersed in the mixed oil sample and

pure olive oil, respectively. A slope of -0.147 ± 0.003 GHz/PU (PU: permittivity unit) can be extracted from Fig. 9(a). That is to say, $\Delta f/\Delta\varepsilon' = -0.147$. As a result, the relative sensitivity of the proposed microwave sensor yields 6.16%.

In addition, the introduction of the MS-CSRR structure in the ground plane makes the microwave patch sensor electrically very small. A comparison between the proposed microwave patch sensor and state-of-the-art microwave sensors is presented in Table 3. It is evident that the proposed sensor in this study offers several key advantages. Specifically, it achieves a notably high sensitivity of 6.16% while maintaining an electrically small size and offers a full-scale detection range (0%–100%). Compared with structurally similar sensors utilizing FR4 substrates, the proposed design demonstrates a significant improvement in sensitivity.

The present experiment mainly focuses on the detection of adulteration in olive oil, but the presented microwave patch sensor can also be used for quality detection of other plant oils, because the fundamental sensing mechanism is based on the variation of dielectric properties induced by different constituent components. Furthermore, implementation of the microwave patch sensor requires only a portable VNA for S-parameter measurement, making the sensing technique suitable for in situ analysis.

5. CONCLUSIONS

In this paper, a high-sensitivity patch antenna-based microwave sensor is proposed for the detection of adulteration in olive oil. The proposed microwave patch sensor has a very high sensitivity, compact size, and a wide detection range of adulteration ratios. The detection of adulteration is easy to carry out by immersing the microwave sensor in the sample under test. Although the main emphasis of this study is limited to the detection of adulteration of corn oil in parent olive oil at room temperature, the proposed microwave patch sensor can be deployed to monitor the adulteration of other plant oils in parent olive oil at other ambient temperatures once the dielectric functions of the mixed oil are established over a wide temperature range. Hence, the proposed methodology for the detection of adulteration in edible oils can easily eliminate the influence of environmental factors, such as temperature, on the detection accuracy. These attractive features make the proposed microwave patch sensor a potential candidate for the real-time quality monitoring of edible oils and noninvasive permittivity measurement of industrial oils. A systematic investigation, including an assessment of its applicability to food safety, is planned for future work.

ACKNOWLEDGEMENT

This work was supported in part by the National Natural Science Foundation of China under Grant No. 62301262 and in part by the Natural Science Foundation of Jiangsu Province of China under Grant No. BK20220440.

REFERENCES

[1] Reboredo-Rodríguez, P., A. Varela-López, T. Y. Forbes-Hernández, M. Gasparrini, S. Afrin, D. Cianciosi, J. Zhang, P. P. Manna, S. Bompadre, J. L. Quiles, M. Battino, and F. Giampieri, "Phenolic compounds isolated from olive oil as nutraceutical tools for the prevention and management of cancer and cardiovascular diseases," *International Journal of Molecular Sciences*, Vol. 19, No. 8, 2305, Aug. 2018.

[2] Al-Ismail, K. M., A. K. Alsaed, R. Ahmad, and M. Al-Dabbas, "Detection of olive oil adulteration with some plant oils by GLC analysis of sterols using polar column," *Food Chemistry*, Vol. 121, No. 4, 1255–1259, Aug. 2010.

[3] Dou, X., J. Mao, L. Zhang, H. Xie, L. Chen, L. Yu, F. Ma, X. Wang, Q. Zhang, and P. Li, "Multispecies adulteration detection of camellia oil by chemical markers," *Molecules*, Vol. 23, No. 2, 241, 2018.

[4] Yildiz Tiryaki, G. and H. Ayvaz, "Quantification of soybean oil adulteration in extra virgin olive oil using portable raman spectroscopy," *Journal of Food Measurement and Characterization*, Vol. 11, No. 2, 523–529, 2017.

[5] Klinar, M., M. Benković, T. Jurina, A. J. Tušek, D. Valinger, S. M. Tarandek, A. Prskalo, J. Tonković, and J. G. Kljusurić, "Fast monitoring of quality and adulteration of blended sunflower/olive oils applying near-infrared spectroscopy," *Chemosensors*, Vol. 12, No. 8, 150, Aug. 2024.

[6] Ge, F., C. Chen, D. Liu, and S. Zhao, "Rapid quantitative determination of walnut oil adulteration with sunflower oil using fluorescence spectroscopy," *Food Analytical Methods*, Vol. 7, No. 1, 146–150, 2014.

[7] Huang, Z.-M., J.-X. Xin, S.-S. Sun, Y. Li, D.-X. Wei, J. Zhu, X.-L. Wang, J. Wang, and Y.-F. Yao, "Rapid identification of adulteration in edible vegetable oils based on low-field nuclear magnetic resonance relaxation fingerprints," *Foods*, Vol. 10, No. 12, 3068, Dec. 2021.

[8] Apetrei, I. M. and C. Apetrei, "Detection of virgin olive oil adulteration using a voltammetric e-tongue," *Computers and Electronics in Agriculture*, Vol. 108, 148–154, Oct. 2014.

[9] Sudhakar, A. and S. K. Chakraborty, "Development of a capacitive sensor-based device for rapid assessment of adulteration in mustard oil," *IEEE Sensors Journal*, Vol. 25, No. 12, 22 554–22 561, Jun. 2025.

[10] Hasar, U. C., H. Korkmaz, H. Hasar, H. Ozturk, and O. Gokgoz, "Detection of storage container and temperature effects in extra virgin olive oil by a sensitive microwave sensor in transmission mode," *IEEE Sensors Journal*, Vol. 25, No. 19, 36 113–36 120, Oct. 2025.

[11] Jasim, H., A. A. Al-Behadili, and S. Ahmed, "Highly sensitive microstrip patch sensor for water salinity monitoring," *Progress In Electromagnetics Research C*, Vol. 157, 247–257, 2025.

[12] De Andrade Lira, R. V., C. R. Freire, I. B. T. Da Silva, V. P. da Silva Neto, J. G. D. de Oliveira, H. D. de Andrade, and A. L. P. de Siqueira Campos, "A compact csrr-based microwave sensor for soil water content," *Sensors and Actuators A: Physical*, Vol. 370, 115211, May 2024.

[13] Hosseinzadeh, S. and M. Pakvarjouy, "Microwave-based single port glucose sensor arranging interdigital and complementary split ring resonator," *Measurement*, Vol. 246, 116695, Mar. 2025.

[14] Kusumah, M. N., S. Alam, I. Surjati, L. Sari, Y. K. Ningsih, F. K. Sari, T. Firmansyah, N. A. Shairi, and Z. Zakaria, "Low-frequency dual-port microwave sensor based on CSRR and electric field coupled for precise permittivity detection in biological

samples," *Progress In Electromagnetics Research M*, Vol. 134, 87–98, 2025.

[15] Chahadih, A., P. Y. Cresson, Z. Hamouda, S. Gu, C. Mismer, and T. Lasri, "Microwave/microfluidic sensor fabricated on a flexible kapton substrate for complex permittivity characterization of liquids," *Sensors and Actuators A: Physical*, Vol. 229, 128–135, Jun. 2015.

[16] Juan, C. G., K. Grenier, M. H. Zarif, A. Ebrahimi, and F. Martin, "Planar microwave sensors: State of the art and applications," *IEEE Access*, Vol. 13, 143 985–144 038, 2025.

[17] Sharafadinzadeh, N., M. Abdolrazzaghi, and M. Daneshmand, "Investigation on planar microwave sensors with enhanced sensitivity from microfluidic integration," *Sensors and Actuators A: Physical*, Vol. 301, 111752, Jan. 2020.

[18] Abdolrazzaghi, M., V. Nayyeri, and F. Martin, "Techniques to improve the performance of planar microwave sensors: A review and recent developments," *Sensors*, Vol. 22, No. 18, 6946, Sep. 2022.

[19] Tiwari, N. K., S. P. Singh, and M. J. Akhtar, "Novel improved sensitivity planar microwave probe for adulteration detection in edible oils," *IEEE Microwave and Wireless Components Letters*, Vol. 29, No. 2, 164–166, Feb. 2019.

[20] Galindo-Romera, G., F. J. Herraiz-Martínez, M. Gil, J. J. Martínez-Martínez, and D. Segovia-Vargas, "Submersible printed split-ring resonator-based sensor for thin-film detection and permittivity characterization," *IEEE Sensors Journal*, Vol. 16, No. 10, 3587–3596, May 2016.

[21] Raveendran, A. and S. Raman, "Low cost multifunctional planar RF sensors for dielectric characterization and quality monitoring," *IEEE Sensors Journal*, Vol. 21, No. 21, 24 056–24 065, Nov. 2021.

[22] Li, Z., C. Wu, Z. Meng, Z. Chen, and F. Fei, "Compact multifunctional five-wire line-based microwave sensor for volumetric characterization of liquids," *IEEE Sensors Journal*, Vol. 22, No. 7, 6566–6575, Apr. 2022.

[23] Alarcon, J. C. P., M. I. O. Souza, V. M. Pepino, and B.-H. V. Borges, "Identification and quantification of common adulterants in extra virgin olive oil using microwave dielectric spectroscopy aided by feedforward neural networks," *IEEE Sensors Journal*, Vol. 24, No. 19, 29 985–29 995, Oct. 2024.

[24] Yin, B. and J. Yin, "Antenna sensor based on an inter-digital capacitor shape EBG structure for liquid dielectric measurement," *Progress In Electromagnetics Research C*, Vol. 140, 65–73, 2024.

[25] Chuma, E. L., Y. Iano, G. Fontgalland, and L. L. B. Roger, "Microwave sensor for liquid dielectric characterization based on metamaterial complementary split ring resonator," *IEEE Sensors Journal*, Vol. 18, No. 24, 9978–9983, Dec. 2018.

[26] Withayachumnankul, W., K. Jaruwongrungsee, A. Tuantranont, C. Fumeaux, and D. Abbott, "Metamaterial-based microfluidic sensor for dielectric characterization," *Sensors and Actuators A: Physical*, Vol. 189, 233–237, 2013.

[27] Han, X., Y. Zhou, X. Li, Z. Ma, L. Qiao, C. Fu, and P. Peng, "Microfluidic microwave sensor loaded with star-slotted patch for edible oil quality inspection," *Sensors*, Vol. 22, No. 17, 6410, Aug. 2022.

[28] Chuma, E. L. and T. Rasmussen, "Metamaterial-based sensor integrating microwave dielectric and near-infrared spectroscopy techniques for substance evaluation," *IEEE Sensors Journal*, Vol. 22, No. 20, 19 308–19 314, Oct. 2022.

[29] Xu, H., W.-J. Wu, W.-S. Zhao, W. Tang, and L. Sun, "Ultrasensitive edible oil sensor based on spiral SLSP combined with stepped structure," *IEEE Transactions on Instrumentation and Measurement*, Vol. 73, 1–9, 2024.

[30] Islam, M. R., M. T. Islam, M. Salaheldeen, B. Bais, S. H. A. Almalki, H. Alsaif, and M. S. Islam, "Metamaterial sensor based on rectangular enclosed adjacent triple circle split ring resonator with good quality factor for microwave sensing application," *Scientific Reports*, Vol. 12, No. 1, 6792, Apr. 2022.

[31] Bhatti, M. H., M. A. Jabbar, M. A. Khan, and Y. Massoud, "Low-cost microwave sensor for characterization and adulteration detection in edible oil," *Applied Sciences*, Vol. 12, No. 17, 8665, Aug. 2022.

[32] Banerjee, A., N. K. Tiwari, F. Fatima, and M. J. Akhtar, "An improved microwave sensor for qualitative assessment of recycled cooking oils," *IEEE Transactions on Instrumentation and Measurement*, Vol. 72, 1–14, 2023.

[33] Beria, Y., G. S. Das, A. Buragohain, P. P. Kalita, and T. Doloi, "Sensitivity enhancement enabled by strongly coupled DG-IDC structure with CSRR for permittivity detection," *IEEE Sensors Journal*, Vol. 25, No. 12, 21 503–21 511, Jun. 2025.

[34] Ali, U., A. Jabbar, X. Yi, M. A. Naveed, M. Q. Mehmood, M. Zubair, and Y. Massoud, "A novel fractal hilbert curve-based low-cost and highly sensitive microwave sensor for dielectric characterization of liquid materials," *IEEE Sensors Journal*, Vol. 23, No. 20, 23 950–23 957, Oct. 2023.

[35] Khalil, M. A., W. H. Yong, M. S. Islam, A. Hoque, L. Y. Chiong, C. C. Leei, H. Alsaif, and M. T. Islam, "A compact tri-octagonal negative indexmetamaterial sensor for liquid adulteration detection," *Optics & Laser Technology*, Vol. 184, 112499, Jun. 2025.

[36] Viskadourakis, Z., A. Theodosi, K. Katsara, M. Sevastaki, G. Fanourakis, O. Tsilipakos, V. M. Papadakis, and G. Kenanakis, "Engraved split-ring resonators as potential microwave sensors for olive oil quality control," *ACS Applied Electronic Materials*, Vol. 6, No. 5, 3846–3856, May 2024.

[37] Han, X., K. Liu, S. Zhang, P. Peng, C. Fu, L. Qiao, and Z. Ma, "CSRR metamaterial microwave sensor for measuring dielectric constants of solids and liquids," *IEEE Sensors Journal*, Vol. 24, No. 9, 14 167–14 176, 2024.

[38] Jiang, S., G. Liu, M. Wang, Y. Wu, and J. Zhou, "Design of high-sensitivity microfluidic sensor based on CSRR with interdigital structure," *IEEE Sensors Journal*, Vol. 23, No. 16, 17 901–17 909, 2023.

[39] Xie, H., W.-J. Wu, W.-S. Zhao, and W. Wang, "A differential microwave sensor based on modified high-sensitivity substrate integrated waveguide (SIW) for detecting glucose concentration in aqueous solution," *IEEE Sensors Journal*, Vol. 25, No. 10, 16 998–17 010, 2025.

[40] Lizhi, H., K. Toyoda, and I. Ihara, "Dielectric properties of edible oils and fatty acids as a function of frequency, temperature, moisture and composition," *Journal of Food Engineering*, Vol. 88, No. 2, 151–158, 2008.

[41] Bakam Nguenouho, O. S., A. Chevalier, B. Potelon, J. Benedicto, and C. Quendo, "Dielectric characterization and modelling of aqueous solutions involving sodium chloride and sucrose and application to the design of a bi-parameter RF-sensor," *Scientific Reports*, Vol. 12, No. 1, 7209, May 2022.

[42] Cataldo, A., E. Piuzzi, G. Cannazza, E. D. Benedetto, and L. Tarricone, "Quality and anti-adulteration control of vegetable oils through microwave dielectric spectroscopy," *Measurement*, Vol. 43, No. 8, 1031–1039, 2010.